1 Covalent Functionalization of Melt-Blown Polypropylene Filters

2 with Diazirine–Photosensitizer Conjugates Producing Visible Light

3 Driven Virus Inactivating Materials.

4 *Authors*: T.J. Cuthbert*[1,2], S. Ennis[3], S. F. Musolino[4], H. L. Buckley[5], M. Niikura[3], J.E.

5 Wulff[4], C. Menon[1,2]

6 Address:[1] Department of Health Sciences and Technology, ETH Zürich, Zürich, 8008,

7 Switzerland; [2] Schools of Mechatronic Systems Engineering & Engineering Science,

8 Simon Fraser University, Metro Vancouver, BC V5A 1S6, Canada; [3] Faculty of Health

9 Sciences, Simon Fraser University, Burnaby, BC V5A 1S6, Canada [4] Department of

10 Chemistry, University of Victoria, Victoria, BC, V8W 3V6, Canada; [5] Department of Civil

11 Engineering, University of Victoria, BC, V8W 3V6, Canada

12 *Email: tyler.cuthbert@hest.ethz.ch

13 Date: March 2021

14 **Abstract**

15 The SARS-CoV-2 pandemic has highlighted the weaknesses of relying on single-use

16 mask and respirator personal protective equipment (PPE) and the global supply chain

17 that supports this market. There have been no major innovations in filter technology for

18 PPE in the past two decades. Non-woven textiles used for filtering PPE are single-use

19   products in the healthcare environment; use and protection is focused on preventing

20   infection from airborne or aerosolized pathogens such as Influenza A virus SARS-CoV-

21   2. Recently, C–H bond activation under mild and controllable conditions was reported

22   for crosslinking commodity aliphatic polymers such as polyethylene and polypropylene.

23   Significantly, these are the same types of polymers used in PPE filtration systems. In

24   this report, we take advantage of this C–H insertion method to covalently attach a

25   photosensitizing zinc-porphyrin to the surface of a melt-blow non-woven textile filter

26   material. With the photosensitizer covalently attached to the surface of the textile,

27   illumination with visible light was expected to produce oxidizing $^1O_2$/ROS at the surface

28   of the material that would result in pathogen inactivation. The filter was tested for its

29   ability to inactivate Influenza A virus, an enveloped RNA virus similar to SARS-CoV-2,

30   over a period of four hours with illumination of high intensity visible light. The

31   photosensitizer-functionalized polypropylene filter inactivated our model virus by

32   99.99% in comparison to a control.

ToC Image
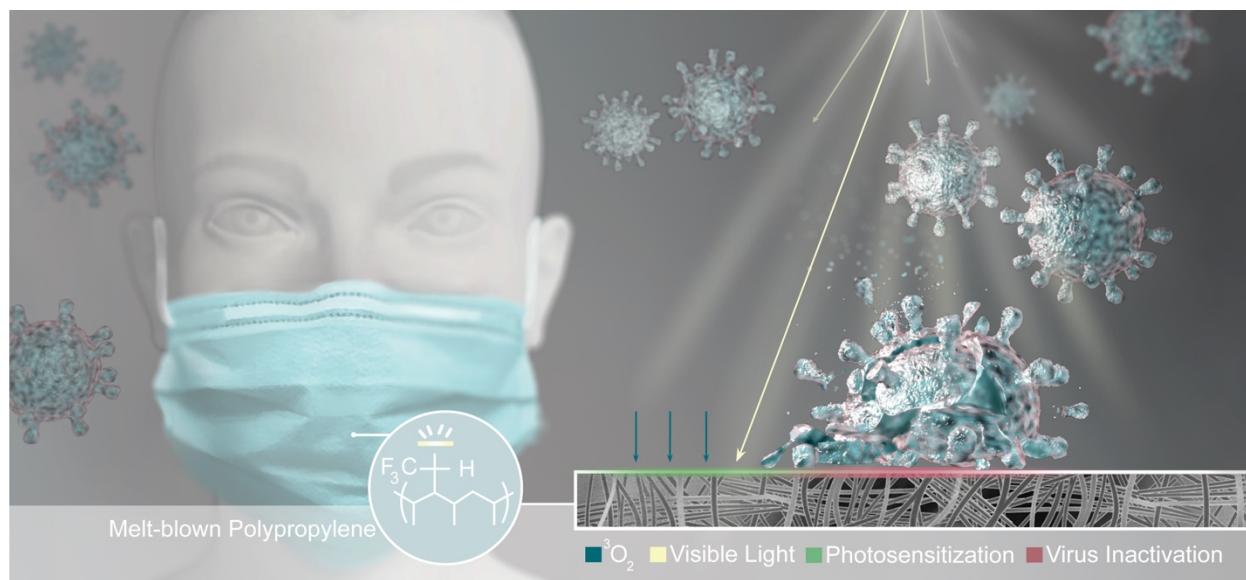
Introduction

The increase in global demand of filter materials for personal protective equipment (PPE) from the SARS-CoV-2 pandemic has highlighted the weakness of the global supply chain and presented the imminent possibility of a limited supply for those that require PPE to complete their job without an undue risk of (self-)infection.[1,2] Potential solutions have been explored to allow PPE reuse in circumstances where supply is not able to keep up with demand. Thus far, the main approaches have focused on treating contaminated materials to inactivate any pathogens captured by the filter. These solutions use available sterilization processes including heat, steam, ethylene oxide, hydrogen peroxide vapour, UV-C, microwaves, salt, and photosensitizers.[3–8] The research using currently available sterilization processes has focused on the number of

46   cycles before device failure, a timely procedure for practicality, and additional health

47   risks—which for sterilization using ethylene oxide is currently in conflict.[4,9] Developing

48   safe, reliable, and reusable filtering materials for PPE remains a challenge. Ideally,

49   sterilizing should not require specialized equipment in order to improve access for

50   healthcare workers and remote communities during times of global supply chain

51   disruption and PPE shortages. In addition, there is potential to decrease the

52   environmental impact of this large industry producing billions of single-use products per

53   year that cannot be recycled. Finally, reports suggest contaminated surfaces and

54   materials are able to produce aerosolized fomites (non-respiratory particles aerosolized

55   from virus-contaminated surfaces) that are capable of spreading disease; specifically, it

56   was hypothesized the aerosolized fomites were originating during removal of

57   contaminated PPE.[10–12]

58   An alternative approach to PPE reuse is to modify the base materials. Ideally, the

59   materials possess filtering, continuous pathogen inactivation, and the ability to self-

60   sterilize when exposed to a plentiful and accessible stimulus. Light is a stimulus that is

61   abundant from both natural and synthetic sources, accessible, and relatively low in cost.

62   Photodynamic therapy (PDT) is a technology that utilizes light (including within the

63   visible spectrum) and photosensitizing (PS) molecules to eradicate pathogens, reduce

64   infection, or eliminate unwanted or cancerous tissue through the production and

65   reaction of singlet oxygen ($^1O_2$) and/or reactive oxygen species (ROS).[13,14] PDT has

66   been used extensively *in vivo* and can be used without causing undue bodily harm.[14]

67   When illuminated with visible light the photosensitizer is excited and proceeds through

68 an energy transfer process with abundant triplet oxygen ($^3O_2$) to produce $^1O_2$ and ROS

69 locally that can be used to eliminate pathogens. The activity is non-specific and can

70 eliminate resistant pathogens that are typically difficult to eradicate.[15–17] As an added

71 benefit, pathogens cannot evolve resistance to $^1O_2$ as easily as they can to small

72 molecule inhibitors.[15,17]

73 Polymer composites, natural and synthetic polymers, and silica particles have been

74 covalently functionalized with photosensitizing molecules and used for microbial

75 inactivation, with the majority of applications focusing on bacterial inactivation.[18] Non-

76 covalent impregnation of photosensitizers into bulk polymer matrices has also been

77 demonstrated to result in microbial inactivation,[19] but the lack of covalent attachment

78 within these systems may lead to leaching of the photosensitizer into the environment.

79 As a result, larger concentrations of the additive will be required in order to avoid a

80 decrease in surface concentration—and therefore activity—over time. Furthermore, the

81 leaching of active components can impact human and environmental health.

82 Covalent attachment approaches have the advantage of reducing the possibility of

83 active component release (leaching) which would inevitably result in a decrease in

84 performance over time. In addition, covalent attachment of photosensitizers can allow

85 the surface of a material to be modified without affecting the bulk. This places the

86 photosensitizer where it is needed (since only the surface of a material can interact with

87 pathogens), thereby requiring less agent to achieve a desired response. In addition, the

88 bulk properties of the substrate material (e.g. tensile strength or glass transition

89 temperature) will be left unperturbed.

90   Rose Bengal, methylene blue, ruthenium-based complexes, pthalocyanines, and

91   porphyrins have been covalently attached to natural and synthetic polymers that bear

92   suitable chemical functionality to support the occurrence of chemical reactions at their

93   surface.[20–29] These covalent attachment methods have been specifically designed for

94   high-functionality materials that are not typically used in PPE/healthcare settings, or

95   else require material pre-functionalization to allow 'click chemistry' (i.e. azide-alkyne

96   coupling through Huisgen cycloadditions). A general solution for attaching

97   photosensitizing molecules onto non-functional materials, such as aliphatic polymers

98   used in PPE for example, remains an obstacle. These types of materials are comprised

99   entirely of C–C and C–H bonds, and therefore lack any chemical "handles" that can be

100   used for derivatization with photosensitizers.

101   One of our research groups recently described a family of *bis*-diazirine reagents that

102   can be used to crosslink simple aliphatic polymers like polyethylene and

103   polypropylene.[30,31] The reagents work by expelling nitrogen gas (N_2) from the tethered

104   diazirine groups upon thermal or photochemical stimulation, to afford high-energy

105   carbenes can then undergo rapid and nearly barrierless insertion any available C–H

106   bonds. In principle, such a technique can also be used to add functionality to base

107   polymeric materials: the desired functional group can simply be tethered to one or more

108   diazirine units, and the resulting conjugate can then be irreversibly linked to the surface

109   of any polymeric material through appropriate activation of the diazirine function.

110   Herein, we employ this C–H activation strategy to permit the covalent functionalization

111   of non-woven melt-blown polypropylene textiles with a common photoactive molecule

112   (Fig. 1). Melt-blown polypropylene (**MBPP**) is a low-functionality polymer that serves as

113   the main filtering component of surgical masks and N95/PAPR respirators. The lack of

114   functional groups in this material means that it cannot be derivatized by traditional

115   covalent linking methods. As a proof of concept, we demonstrated the inactivation of

116   influenza A virus (IFV) using a visible light stimulus. IFV was chosen as a model

117   because IFV itself is a major threat as a potential pandemic virus, and because IFV's

118   enveloped structure and RNA genome is similar to those of SARS-CoV-2—the

119   organism that is the proximal cause of the current pandemic. Researchers have

120   indicated previously the importance of developing and testing inactivation methods

121   against enveloped viruses, given that a pandemic was expected long before the

122   emergence of SARS-CoV-2.[32]
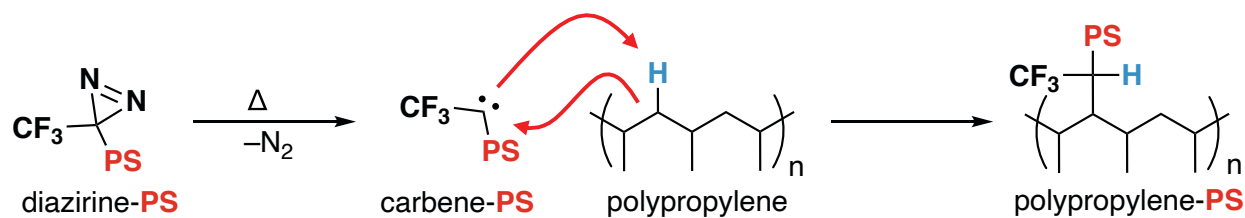
PS = Photosensitizer (zinc-porphyrin)

123

124   Figure 1. Strategy for creating covalently functionalized aliphatic polymer filters using

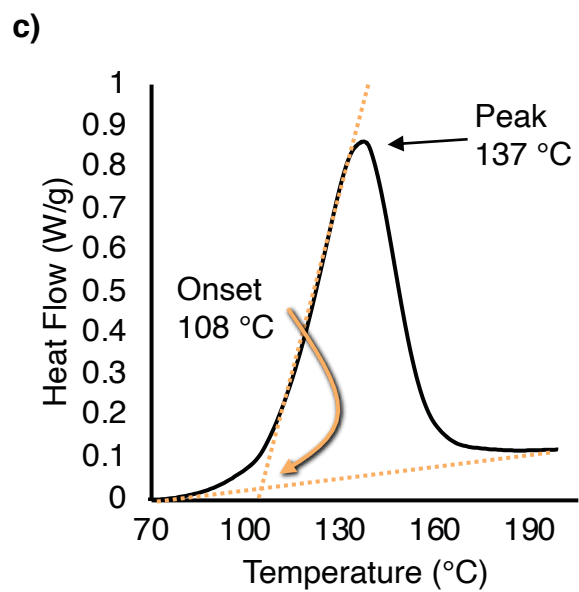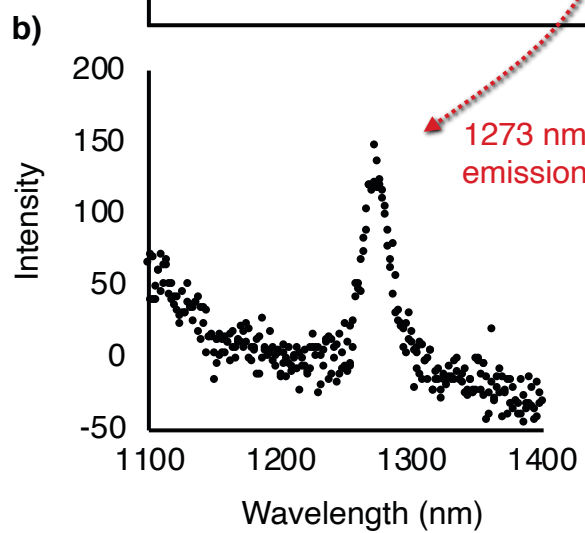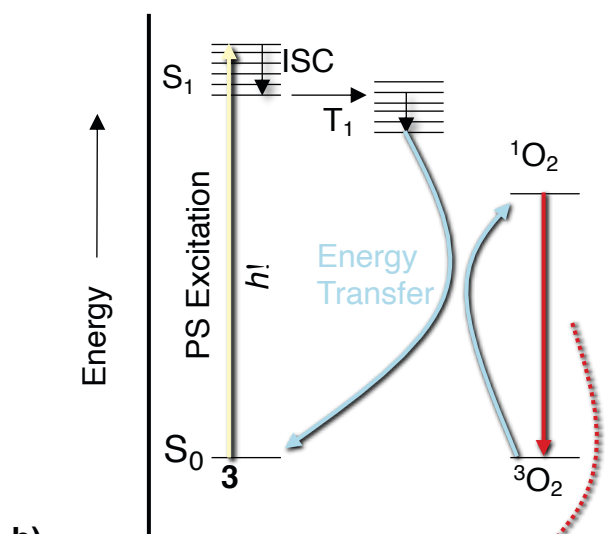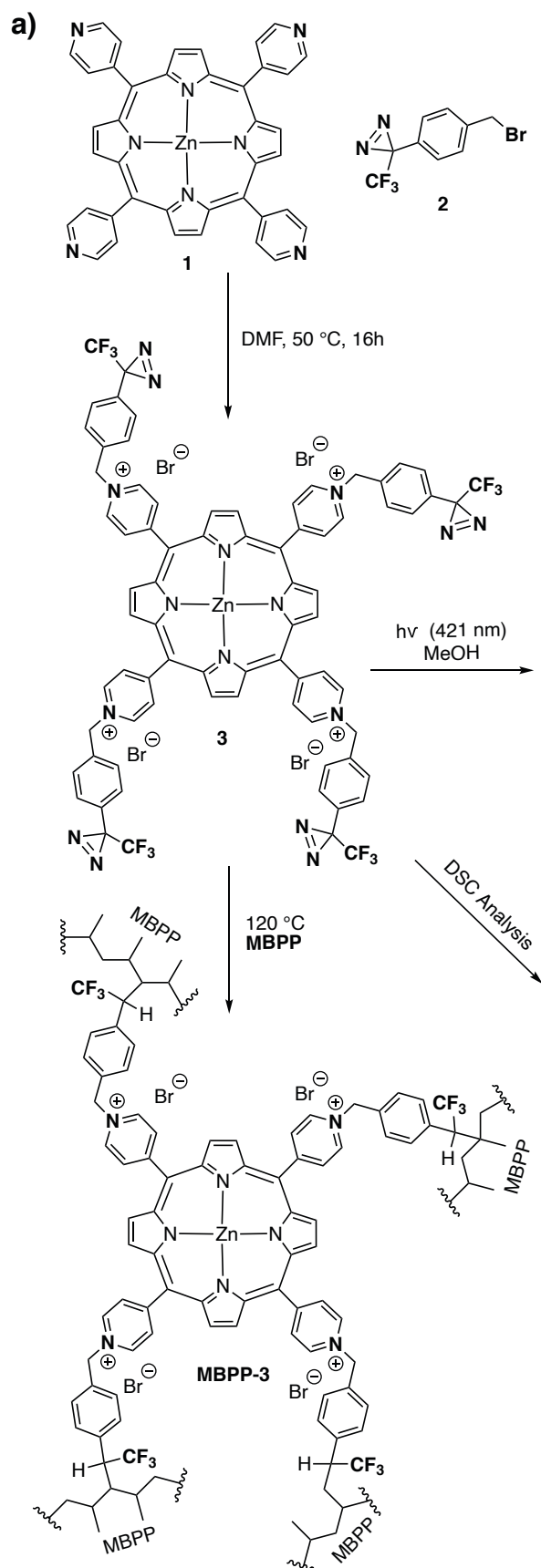125   diazirine C–H insertion chemistry and photosensitizers.

126   ## Results and Discussion

127   **Functionalization of non-woven polypropylene filter with photoactive porphyrin**

128 The **MBPP** substrate was chosen because of the widespread use of the non-woven

129 material in filtering PPE, specifically single-use surgical masks and N95/personal air

130 purifying respirators. A commercially available photosensitizer (**1**) was selected, which

131 possessed a high quantum yield for the production of singlet oxygen with visible light,

132 and which possessed nucleophilic residues for easy derivatization. To facilitate insertion

133 into the surface accessible C–H bonds of the **MBPP**, we utilized a 3-trifluoromethyl-3-

134 phenyl-3*H*-diazirine motif (TFMPD) that is known to generate carbenes that are capable

135 of ready insertion into C–H bonds.[33] A commercially available benzyl bromide (**2**) that

136 incorporates the TFMPD motif was reacted with the pyridyl groups of **1** to produce the

137 desired tetrakis diazirinyl zinc-porphyrin **3** in near-quantitative yield (Fig. 2a). We

138 confirmed $^1O_2$ production with fluorescence spectroscopy from the excitation of **3** and

139 subsequent phosphorescence of $^1O_2$ at 1273 nm. The $^1O_2$ generation proceeds through

140 the photoexcitation of ground state **3** (S_0) to generate the singlet excited state of **3** (S_1),

141 intersystem crossing to a triple state **3** (T_3), and then an energy transfer to the triplet

142 ground state of oxygen ($^3O_2$) to produce singlet oxygen ($^1O_2$) which then undergoes

143 phosphorescence back to the ground state observed as an emission at a wavelength of

144 1273 nm indicating that the zinc-porphyrin moiety still possessed activity when

145 functionalized with four diazirine groups (Fig. 2b).

146 The surface of the **MBPP** was then covalently functionalized with **3** using a modified

147 procedure from Lepage et al.[30] To facilitate this, the reactivity of the diazirines in **3** was

148 first analyzed by differential scanning calorimetry (DSC). These data revealed an onset

149 temperature of 108 °C (determined by extrapolation of the tangent of the upward slope

8

150   to the fitted baseline of the plot) and a peak temperature of 137 °C (Fig. 2c). With this

151   information in hand, we chose to react compound **3** with **MBPP** for 4 hours at 120 °C

152   (using 10 wt% of **3** with respect to **MBPP**) to afford **MBPP-3**, a green-coloured textile.

a)

DMF, 50 °C, 16h

hv (421 nm)
MeOH

DSC Analysis

120 °C
MBPP

b)

1273 nm
emission

c)

Peak
137 °C

Onset
108 °C

153

154   Figure 2. a) Synthesis of **3** and subsequent **MBPP** functionalization. b) $^1O_2$

155   phosphorescence after excitation of **3** at 421 nm. c) DSC of **3** indicating the onset and

156   peak reaction temperature of the diazirine.

157   The intense green colour of **3** was advantageous for (1) ensuring coverage of **MBPP**

158   with the solution of **3**, and (2) monitoring the effectiveness of the diazirine C–H insertion

159   reaction through the persistent green colour after washing (Fig. S5). Prior to virus

160   inactivation testing we completed a robust washing protocol analyzing the wash

161   fractions with UV-Vis spectroscopy to observe the removal of **3** that did not covalently

162   react with the surface of **MBPP**. The washing process was initially completed over ~6

163   days with 12 changes in solvent (Fig. S4). It was crucial to ensure complete removal of

164   any **3** that did not covalently bind to **MBPP** during the C–H insertion step to ensure that

165   our subsequent virus inactivation testing focused on the abilities of **MBPP-3** exclusively.

166   The efficacy of free antimicrobials is greater than that of an immobilized antimicrobial

167   because of the ability to diffuse throughout a solution; in the case of an immobilized

168   antimicrobial, the activity is reliant upon virus diffusion to within the proximity of the

169   surface of the material where the interaction/reaction can occur. The lifetime of the

170    $^1O_2$/ROS produced (μs to ms) limits the space in which inactivation may take place

171   which we hypothesized would create layer at and above the material's surface that

172   would inactivate any virus occupying that space.[34,35] The inactivation would then rely on

173   pathogen diffusion in the transfer medium to within this concentrated $^1O_2$ area on the

174   **MBPP-3** surface and was therefore expected to present a time-dependence. Virus

11

175   inactivation testing was then completed using a minimal volume of carrier medium to

176   mimic aerosolized and droplet capture by the filter.

177   IFV (strain A/California/07/2009) was used as a model enveloped RNA virus. IFV would

178   provide insight into the inactivation performance of our material against enveloped RNA

179   viruses similar to the SARS-CoV-2, which continues to cause a worldwide pandemic in

180   2021. We used a high-intensity LED light capable of producing ~30,000 lux to excite

181   **MBPP-3** (see Supplementary Fig. 6 for manufacturer's provided UV-Vis profile) which

182   would mimic the amount of light that may be found in a hospital operating theatre or

183   emergency area.[36]

184   The virus particles were exposed to the light for between 0.5 and 4 hours in 10 μL of

185   tissue culture medium in a well of a 96-well plate that contained a test surface (see

186   Supplementary Fig. 5). After 1 hour exposure the virus titer was reduced by 1.06 log

187   with **MBPP-3**, compared with only a minor 0.13 log reduction on the **MBPP** control

188   surface (Fig. 3a). Over the 4-hour testing period a logarithmic relationship between

189   reduction of PFUs and exposure time was observed. At 4 hours of exposure, the treated

190   surface resulted in a 4.07 log reduction (99.99%) in comparison to an empty well, a 3.38

191   log reduction (99.96%) in comparison to untreated **MBPP** and a 5.95 log reduction

192   (99.9999%) in comparison to the starting virus PFU concentration.
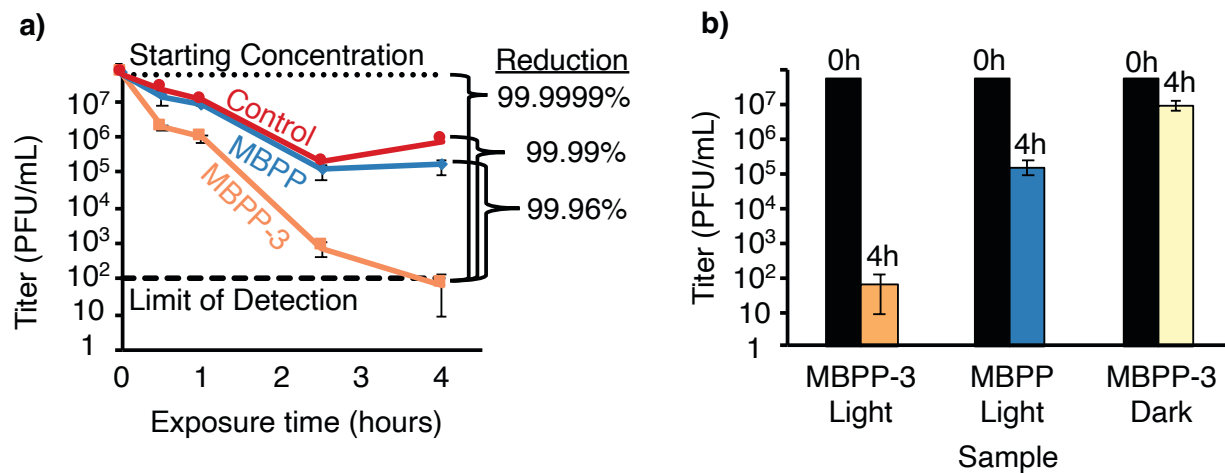
195   Figure 3. a) Log_{10} Reduction of PFU/mL active virus vs. exposure time to visible light

196   against the control (empty well), **MBPP**, and **MBPP-3**; b) Log_{10} Reduction of PFU/mL

197   active virus at 4 hours against **MBPP-3** and **MBPP** with and without light in comparison

198   to the starting virus concentration (0h).

199   These data indicate that near sterilization levels of inactivation may be achievable over

200   longer periods (4+ hours) of high-intensity illumination of **MBBP-3** offering an alternative

201   approach to re-sterilization and re-use of PPE. A distinct advantage of chemically

202   modifying the material is to facilitate continuous sterilization during use, which would

203   decrease the potential for aerosolized fomites when using or removing PPE decreasing

204   a potential mode of infection.[10]

205   To differentiate the impact of immobilized **3** and visible light contribute to the viral

206   inactivation efficacy we completed an analogous virus exposure test of **MBPP-3** in the

207   absence of light (Fig. 3b). Without exposure to light, **MBPP-3** minimally inactivated the

208   inactivated the virus with a 0.76 log reduction (Fig. 3b; **MBPP-3 Dark**), which was

209   substantially less than **MBPP** exposed to light. These data indicated that immobilized **3**

210   and visible light are required to achieve efficient virus inactivation, and that switchable

211   on/off performance and lithography/patterning of virus inactivation may be possible with

212   this system.

213   The ability to functionalize aliphatic polymers with diazirines is a relatively new

214   methodology and has the potential to impact a large portion of the commodity polymer

215   market. Low-functionality aliphatic polymers—such as the MBPP used in this

216   research—account for the largest three (polypropylene, low-density and high-density

217   polyethylene) volumes of thermoplastics in the world equating to ~36% or 23 million

218   tons of polymers used worldwide each year.[34] With over 39% in packaging and 22% in

219   other areas that include health and safety, the potential for improvement in product

220   performance and safety across different markets that utilize aliphatic polymers is high.

221   Furthermore, this method of functionalization can be applied to different commodity

222   polymers including polystyrene or polyethylene terephthalate and as such may allow

223   recycled materials an avenue for use in high-performance and advanced material

224   applications from renewable resources. The diazirine functionality is not limited to C–H

225   bond activation and can also be used to functionalized more reactive O–H and N–H

226   bonds in polyalcohols and polyamides which could be used for post-processing

227   functionalization of different materials that would benefit from self-sterilization in

228   healthcare settings.[30]

229   Future testing will focus on the development of this technology to understand the

230   performance limitations of the material with respect to repeated sequential virus

231   inactivation, potential photobleaching, light intensity-dependent performance, response

232   to washing and detergents, and performance against different types of pathogens. The

233   optimization of inactivation materials should be focused on developing technology that

234   is broadly applicable, robust, and possesses broad spectrum activity without the

235   potential for developing resistance.

236   Conclusions

237   We have described the production of a polypropylene-based non-woven filter that was

238   covalently functionalized with a zinc-porphyrin photosensitizer using diazirine C–H

239   activation chemistry. The **MBPP-3** material was tested against a model virus, Influenza

240   A, to explore the virus inactivation abilities of the material when exposed to visible light.

241   Over a 4-hour incubation period with exposure to visible light there was 4-log reduction

242   of active virus resulting in a logarithmic trend in the inactivation of virus over time, and a

243   5.95 log reduction in comparison to the starting virus concentration. This research

244   presents a new approach to achieving functionalized aliphatic polymers, such as those

245   used in PPE, which provides a potential solution for reducing pathogen transfer; a route

246   for designing re-useable and re-sterilizable PPE that can reduce the need for single-use

247   products; and the development of post-functionalization processes that could see

248   widespread use across many different forms of PPE.

Methods

All chemicals were used as received. Zinc 5,10,15,20-*tetra*(4-pyridyl)-21*H*,23*H*-porphine was purchased from Sigma Aldrich (Missouri, USA). 4-[3-(trifluoromethyl)-3*H*-diazirin-3-yl]benzyl bromide was purchased from TCI America (Portland, USA). Melt-blown polypropylene was supplied by Epic Ventures Inc (Victoria, Canada) EM-X090 LED light with incorporated driver (90W) was purchased from Jons Plant Factory (Burnaby, Canada). Illuminance (luminous flux/unit area, lux = lumens/m^2) was measured with the Lux Light Meter app using an Apple iPhone. For experimental virus inactivation and LED light setup see Supplementary Fig. 5. Fluorescence spectroscopy measurements were completed on a Horiba Jobin Yvon Fluorolog-3 fluorimeter equipped with an Xe arc lamp and a TBX single-photon counter in a quartz cuvette.

Synthesis of tetra diazirine zinc porphyrin (3)

Zinc 5,10,15,20-*tetra*(4-pyridyl)-21*H*,23*H*-porphine (ZnTPyP, **1**) (70 mg, 0.102 mmol) was dissolved in 2 mL of DMF, then 4-[3-(trifluoromethyl)-3*H*-diazirin-3-yl]benzyl bromide (**2**) (171 mg, 0.61 mmol) was added to the solution and the reaction was heated to 50°C and stirred vigorously for 16 h. The solvent was then evaporated under reduced pressure and the crude product **3** (211 mg, 0.10 mmol, 99%) was obtained as dark green solid. ^{1}H NMR (300 MHz, MeOD) δ 9.49 (d, *J* = 6.6 Hz, 8H), 9.15 (s, 8H), 8.95 (d, *J* = 6.7 Hz, 8H), 8.01 (d, *J* = 8.5 Hz, 8H), 7.55 (d, *J* = 7.9 Hz, 8H), 6.31 (s, 8H). ^{13}C NMR (126 MHz, MeOD) δ 164.88, 161.79, 150.37, 144.22, 136.60, 134.69, 134.03, 131.81, 131.62, 130.87, 129.74, 128.94, 128.38, 123.50 (q, *J* = 273.9 Hz), 117.30,

270   64.82, 37.00, 35.40, 32.55, 31.68, 29.45 (q, $J = 40.7$ Hz). ^{19}F NMR (283 MHz, MeOD) δ

271   —66.90.

Production of zinc porphyrin functionalized melt-blown polypropylene (MBPP-3)

273   **MBPP** was cut into 4 cm diameter circles (with an initial white colour) and placed in 4

274   cm diameter aluminum weigh boats. Each MBPP piece was submerged in a methanol

275   solution of **3** (equating to a concentration of **3** that was 10 wt% of the **MBPP** textile) and

276   was subsequently covered with aluminum foil and allowed to incubate at room

277   temperature for 1 hour. The aluminum pans containing the **MBPP** and **3** were then

278   uncovered and the methanol solvent was allowed to evaporate in the dark for 4 hours

279   which resulted in a green coloured **MBPP** textile. The pans containing **MBPP** and **3**

280   were then incubated for 4 hours at 120°C in an oven. The resulting **MBPP-3** textile was

281   then washed with ethanol to remove any residual non-bound **3** by incubating the textile

282   in 10 mL (first 10 washings) then 500 mL (last two washings) of ethanol until no

283   remaining **3** was observed by UV-Vis spectroscopy. The **MBPP-3** textiles were then air

284   dried and used for virus inactivation testing.

Virus Inactivation Testing

286   **MBPP-3** was punched to precisely fit the bottom of a 96-well plate, soaked in 70%

287   ethanol for 10 minutes, and air dried prior to testing. **MBPP** and **MBPP-3** were tested

288   with 9 replicates and controls (empty wells) were completed in triplicate. Influenza A

289   virus (A/California/07/2009 (H1N1)pdm09 virus, International Reagent Resources) in

290   Dulbecco's Modified Eagle medium (DMEM, 10 μL) was added to each well at a

17

291   concentration of 5.98x10^7 plaque forming unit (PFU)/mL. The plate was exposed for

292   the indicated time to visible light (31,951-30,198 lux at the 96-well plate) or wrapped

293   with aluminum foil for the dark/no light exposure experiment) with a temperature range

294   between 24 (start) to 30.2 °C (end). Following exposure, 50 μL phosphate buffered

295   saline (PBS) was added to resuspend remaining viruses from the wells and pooled in

296   triplicates, resulting in 3 samples each from **MBPP-3** and **MBPP** containing wells, and 1

297   sample for negative control. The samples were split into aliquots and stored at –80 °C

298   until use. Viruses titers were then determined in 10-fold serial dilutions on MDCK

299   (ATCC) in plaque assays. Antiviral efficacy was calculated by counting the number of

300   remaining plaques.

301   **Acknowledgements**

306   **Author Contributions**

307   J.W. and H.B. designed compound **3** for use in pathogen inactivation at polymer

308   surfaces. S.M. synthesized compound **3**. T.C. carried out the singlet oxygen studies,

309   applied the diazirine conjugate to the polymer surface, and confirmed covalent

310   attachment though repetitive extraction. S.E. and M.N. conducted the antiviral

311 experiments. T.C. wrote the manuscript, while working under the supervision of C.M.,

312 with input from all authors.

313 **Competing Interests**

314 S.M., H.B., and J.W. are co-inventors on PCT/CA2021/050290, which claims the use of

315 porphyrin–diazirine conjugate **3**. The authors declare no additional competing interests.

316 **References**

317 1. Howard, J. *et al.* An evidence review of face masks against COVID-19. *Proc. Natl.*

318   *Acad. Sci.* **118**, e2014564118 (2021).

319 2. Paxton, N. C. *et al.* N95 Respiratory Masks for COVID-19: A Review of the

320   Literature to Inform Local Responses to Global Shortages. *Pre Print* at

321   https://research.qut.edu.au/biofabrication/wp-

322   content/uploads/sites/62/2020/04/N95_COVID-

323   19_LiteratureReview_2020_Submission.pdf (2020).

324 3. de Man, P., van Straten, B., van den Dobbelsteen, J. & van der Eijk, A. Sterilization

325   of disposable face masks by means of standardized dry and steam sterilization

326   processes; an alternative in the fight against mask shortages due to COVID-19. *J.*

327   *Hosp. Infect.* **2**, 356–357 (2020).

328 4. Viscusi, D. J., Bergman, M. S., Eimer, B. C. & Shaffer, R. E. Evaluation of Five

329   Decontamination Methods for Filtering Facepiece Respirators. *Ann. Occup. Hyg.* **53**,

330   815–827 (2009).

331   5. Kumar, A. *et al.* N95 Mask Decontamination using Standard Hospital Sterilization

332   Technologies. *medRxiv* at

333   https://www.medrxiv.org/content/10.1101/2020.04.05.20049346v2 (2020)

334   6. Quan, F.-S., Rubino, I., Lee, S.-H., Koch, B. & Choi, H.-J. Universal and reusable

335   virus deactivation system for respiratory protection. *Sci. Rep.* **7**, 39956 (2017).

336   7. Daeschler, S. C. *et al.* Effect of moist heat reprocessing of N95 respirators on

337   SARS-CoV-2 inactivation and respirator function. *CMAJ* **192,** E1189-E1197 (2020).

338   8. Yao, T. *et al.* A photodynamic antibacterial spray-coating based on the host–guest

339   immobilization of the photosensitizer methylene blue. *J. Mater. Chem. B* **7**, 5089–

340   5095 (2019).

341   9. *Ethylene Oxide Sterilization Systems must not be used to sterilize masks and*

342   *respirators*. https://lni.wa.gov/safety-health/preventing-injuries-

343   illnesses/hazardalerts/MaskCleaning.pdf?utm_medium=email&utm_source=govdeliv

344   ery (2020).

345   10. Asadi, S. *et al.* Efficacy of masks and face coverings in controlling outward aerosol

346   particle emission from expiratory activities. *Sci. Rep.* **10**, 15665 (2020).

347   11. Asadi, S. *et al.* Influenza A virus is transmissible via aerosolized fomites. *Nat.*

348   *Commun.* **11**, 4062 (2020).

349   12. Liu, Y. *et al.* Aerodynamic analysis of SARS-CoV-2 in two Wuhan hospitals. *Nature*

350   **582**, 557–560 (2020).

351   13. Loebel, N. G., Cross, C. M., Meller, D. M., Hickok, J. & Andersen, R. Antimicrobial

352   Photodisinfection Therapy: Essential Technology for Infection Control. *Ondine*

353   *Biomedical Inc White Paper* (2020).

354   14. Breskey, J. D. *et al.* Photodynamic Therapy: Occupational Hazards and Preventative

355   Recommendations for Clinical Administration by Healthcare Providers. *Photomed.*

356   *Laser Surg.* **31**, 398–407 (2013).

357   15. Tavares, A. *et al.* Antimicrobial Photodynamic Therapy: Study of Bacterial Recovery

358   Viability and Potential Development of Resistance after Treatment. *Mar. Drugs* **8**,

359   91–105 (2010).

360   16. Maisch, T. Resistance in antimicrobial photodynamic inactivation of bacteria.

361   *Photochem. Photobiol. Sci.* **14**, 1518–1526 (2015).

362   17. Al-Mutairi, R., Tovmasyan, A., Batinic-Haberle, I. & Benov, L. Sublethal

363   Photodynamic Treatment Does Not Lead to Development of Resistance. *Front.*

364   *Microbiol.* **9**, 1699 (2018).

365   18. Spagnul, C., Turner, L. C. & Boyle, R. W. Immobilized photosensitizers for

366   antimicrobial applications. *J. Photochem. Photobiol. B* **150**, 11–30 (2015).

367   19. Peddinti, B. S. T., Scholle, F., Ghiladi, R. A. & Spontak, R. J. Photodynamic

368   Polymers as Comprehensive Anti-Infective Materials: Staying Ahead of a Growing

369   Global Threat. *ACS Appl. Mater. Interfaces* **10**, 25955–25959 (2018).

370 20. Moczek, L. & Nowakowska, M. Novel Water-Soluble Photosensitizers from

371   Chitosan. *Biomacromolecules* **8**, 433–438 (2007).

372 21. Guo, Y., Rogelj, S. & Zhang, P. Rose Bengal-decorated silica nanoparticles as

373   photosensitizers for inactivation of gram-positive bacteria. *Nanotechnology* **21**,

374   065102 (2010).

375 22. Schaap, A. P., Thayer, A. L., Blossey, E. C. & Neckers, D. C. Polymer-based

376   sensitizers for photooxidations. II. *J. Am. Chem. Soc.* **97**, 3741–3745 (1975).

377 23. Ringot, C. *et al.* Triazinyl Porphyrin-Based Photoactive Cotton Fabrics: Preparation,

378   Characterization, and Antibacterial Activity. *Biomacromolecules* **12**, 1716–1723

379   (2011).

380 24. Ringot, C., Sol, V., Granet, R. & Krausz, P. Porphyrin-grafted cellulose fabric: New

381   photobactericidal material obtained by "Click-Chemistry" reaction. *Mater. Lett.* **63**,

382   1889–1891 (2009).

383 25. Bonnett, R., Krysteva, M. A., Lalov, I. G. & Artarsky, S. V. Water disinfection using

384   photosensitizers immobilized on chitosan. *Water Res.* **40**, 1269–1275 (2006).

385 26. Carpenter, B. L., Feese, E., Sadeghifar, H., Argyropoulos, D. S. & Ghiladi, R. A.

386   Porphyrin-Cellulose Nanocrystals: A Photobactericidal Material that Exhibits Broad

387   Spectrum Antimicrobial Activity†. *Photochem. Photobiol.* **88**, 527–536 (2012).

388 27. Krouit, M., Granet, R. & Krausz, P. Photobactericidal films from porphyrins grafted to

389   alkylated cellulose – synthesis and bactericidal properties. *Eur. Polym. J.* **45**, 1250–

390   1259 (2009).

391 28. Kim, H.-S. *et al.* Antibacterial application of covalently immobilized photosensitizers

392   on a surface. *Environ. Res.* **172**, 34–42 (2019).

393 29. Blacha-Grzechnik, A., Drewniak, A., Walczak, K. Z., Szindler, M. & Ledwon, P.

394   Efficient generation of singlet oxygen by perylene diimide photosensitizers

395   covalently bound to conjugate polymers. *J. Photochem. Photobiol. Chem.* **388**,

396   112161 (2020).

397 30. Lepage, M. L. *et al.* A broadly applicable cross-linker for aliphatic polymers

398   containing C–H bonds. *Science* **366,** 875–878 (2019).

399 31. Simhadri, C. *et al.* Flexible polyfluorinated bis-diazirines as molecular adhesives.

400   *Chem. Sci.* **12,** 4147-4153 (2021)

401 32. Larson, E. L. & Liverman, C. T. Designing and Engineering Effective PPE. in

402   *Institute of Medicine (US) Committee on Personal Protective Equipment for*

403   *Healthcare Personnel to Prevent Transmission of Pandemic Influenza and Other*

404   *Viral Respiratory Infections: Current Research Issues; Larson EL, Liverman CT,*

405   *editors. Preventing Transmission of Pandemic Influenza and Other Viral Respiratory*

406   *Diseases: Personal Protective Equipment for Healthcare Personnel: Update 2010.*

407   (National Academies Press (US), 2011).

408   33. Brunner, J., Senn, H. & Richards, F. M. 3-Trifluoromethyl-3-phenyldiazirine. A new

409   carbene generating group for photolabeling reagents. *J. Biol. Chem.* **255**, 3313–

410   3318 (1980).

411   34. Skovsen, E., Snyder, J. W., Lambert, J. D. C. & Ogilby, P. R. Lifetime and Diffusion

412   of Singlet Oxygen in a Cell. *J. Phys. Chem. B* **109**, 8570–8573 (2005).

413   35. Wang, K.-K. *et al.* Lifetime and diffusion distance of singlet oxygen in air under

414   everyday atmospheric conditions. *Phys. Chem. Chem. Phys.* **22**, 21664–21671

415   (2020).

416   36. Bukorovic, N. *Lighting Guide 2 - Hospitals and Health Care Buildings*. (Chartered

417   Institution of Building Services Engineers, London, 2008).

418